Tectonophysics 583 (2013) 49–53

Contents lists available at SciVerse ScienceDirect

Tectonophysics

journal homepage: www.elsevier.com/locate/tecto

Effect of pore fluid pressure on the frictional strength of antigorite serpentinite

Keishi Okazaki [a],*, Ikuo Katayama [a], Miki Takahashi [b]

[a] Department of Earth and Planetary Systems Science, Hiroshima University, 1-3-1 Kagami-yama, Higashi-Hiroshima, Hiroshima, 739–8526, Japan
[b] Geological Survey of Japan, National Institute of Advanced Industrial Science and Technology (AIST), Tsukuba, Ibaraki, 305–8567, Japan

ARTICLE INFO

Article history:
Received 17 March 2012
Received in revised form 13 October 2012
Accepted 21 October 2012
Available online 30 October 2012

Keywords:
Antigorite serpentinite
Effective pressure
Coulomb's law
Laboratory experiments
Friction coefficient
Slow earthquakes

ABSTRACT

Triaxial deformation experiments on antigorite serpentinite show a systematic correlation between shear stress and effective normal stress over a wide range of pore pressures ($50<P_p<143$ MPa). Under dry conditions using Ar gas as the pore fluid, the steady-state friction coefficient (μ) is estimated to be 0.66 ± 0.01. In contrast, under wet conditions using distilled water as the pore fluid, $\mu=0.51\pm0.01$ (i.e., less than under dry conditions). This difference in μ may be caused by charged water on the serpentine surface, which reduces the frictional resistance of the sliding surface in wet environments. The linear correlation between shear stress and effective normal stress suggests that Coulomb's law applies to sliding surfaces during the injection and ejection of pore fluids. This results in a significant mechanical weakening due to elevated pore fluid pressures; consequently, the locations of asperities on plate boundaries may be controlled by the heterogeneous distribution of fluids on the subducting plate interface.

1. Introduction

Slow earthquakes (e.g., slow slip events, very low frequency earthquakes, and non-volcanic tremors) have been detected in subduction zones where relatively young, hot slabs are subducting, such as southwest Japan, Cascadia, and Costa Rica (Obara, 2002; Rogers and Dragert, 2003; Schwartz and Rokosky, 2007). Most slow earthquakes in subduction zones occur at depths of 30 to 45 km, and are located at the corner of the mantle wedge, slightly deeper than the seismogenic zone of megathrust earthquakes (ca. 30 km) (Obara, 2002; Brown et al., 2009). Low velocity anomalies and high Poisson's ratios have been detected in these regions, suggesting that serpentinite and high pore-fluid pressure play a role in triggering such events (Audet et al., 2009; Matsubara et al., 2009; Peacock et al., 2011; Shelly et al., 2006).

Non-volcanic tremors occur along the San Andreas Fault, and are triggered by the tidal force, even though the tidal force is extremely weak (less than 1 kPa) when compared with the lithostatic pressure at source regions of non-volcanic tremors (Thomas et al., 2009). This means the effective pressure at source regions of non-volcanic tremors is very low, and sufficiently low for tidal stresses to trigger tremors effectively. Nakata et al. (2008) estimated that the effective normal stress at a tremor source region is 100 kPa, indicating that fluid pressure may approach lithostatic pressure. The strong anisotropy in the permeability of serpentinite might result in preferential fluid migration along the subducting plate interface, and the permeability contrast between serpentinite (hydrated mantle) and gabbro (continental crust) along the Moho results in the accumulation of water and the build-up of pore pressure in the mantle wedge corner (Katayama et al., 2012; Kawano et al., 2011). In Northeast Japan, where relatively old and cold slabs are subducting, a high *Vp*/*Vs* ratio is observed in oceanic crust beneath the corner of the mantle wedge, but such a ratio is not observed at the corner of the mantle wedge (Tsuji et al., 2008). In this area, no slow earthquakes are observed, and this might suggest that slow earthquakes require not only a high pore fluid pressure, but also hydration of the corner of a mantle wedge. In other words, fluids and the nature of the materials involved all play important roles in the generation of slow earthquakes.

Slow earthquakes are characterized by a different scaling law to regular earthquakes (Ide et al., 2007), but the physical mechanisms of slow earthquakes are not fully understood. Serpentinites, which are hydrated mantle material, are known to have unique characteristics in terms of friction (e.g., Moore et al., 1997; Morrow et al., 2000; and Takahashi et al., 2011); however, the quantitative influence of pore-fluid pressures on their frictional strength is not well constrained. Consequently, in this study we focus on the effect of pore-fluid pressure on the frictional behavior of serpentinite, and evaluate the potential role of high pore pressure on the asperity model and the enhancement of slow earthquakes at subducting plate interfaces.

2. Experimental details

The experiments were performed on antigorite serpentinite using a gas-medium, high-pressure, high-temperature triaxial deformation apparatus at Hiroshima University, Japan (Fig. 1). The apparatus (for

---

* Corresponding author. Tel.: +81 824 24 7468; fax: +81 824 24 0735.
E-mail address: okazakikeishi@hiroshima-u.ac.jp (K. Okazaki).

0040-1951/$ – see front matter © 2012 Elsevier B.V. All rights reserved.
http://dx.doi.org/10.1016/j.tecto.2012.10.017

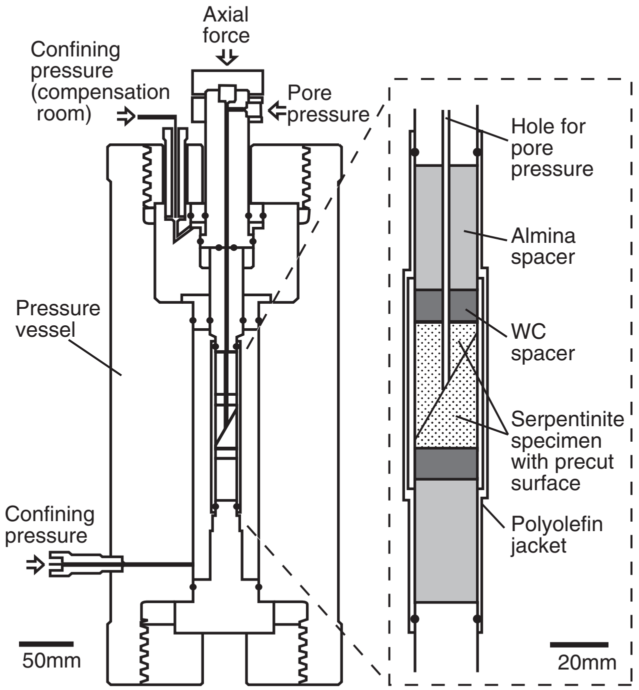

Fig. 1. Cross-section of the pressure vessel and specimen assembly in the gas-medium, high-pressure, high-temperature triaxial deformation apparatus at Hiroshima University. The cylindrical serpentinite sample, with a fault surface oriented at 30° to the maximum compressional axis, was used by advancing an axial piston controlled by a servo-controlled system. Pore fluids were supplied from a small hole in the upper spacer, with argon gas use for the dry experiment, and distilled water for the wet experiments. The specimen assembly and spacers were arranged in three layers of a heat-shrinkable polyolefin jacket, and the strength of the jacket was removed when calculating the sample strength.

details, see Uehara and Shimamoto, 2004; Wibberley and Shimamoto, 2003) consisted of a cylindrical pressure vessel, a pressure-generating system for confining pressure (P_c), and a pore pressure (P_p) intensifier and loading system, and can generate values of P_c and P_p of up to 220 MPa. In this system, the axial load and P_p are controlled by a servo-system with a frequency of 200 Hz.

We used a serpentinite block sampled from the Nomo metamorphic belt, Japan, for these experiments. The sample was completely serpentinized, with no olivine relicts, and consisted predominantly of antigorite (ca. 98%) with a random fabric, and minor diopside, spinel, and magnetite. The serpentinite block was cored and polished to cylindrical specimens (20 mm in diameter and 40 mm long) with oblique fault surfaces oriented at 30° to the cylinder axis. The fault surfaces were polished to a uniform roughness using #80 carborundum. The specimens were dried for more than 24 h at 120 °C in an oven to eliminate any absorbed water from the surface.

Fig. 1 shows a schematic diagram of the pressure vessel and specimen assembly. Argon gas was used as the confining-pressure medium, and distilled water as a pore-pressure medium, except in experiment GR623, which was a dry experiment with argon gas used as the pore fluid. The specimen assembly and spacers were placed into three layers of a heat-shrinkable polyolefin jacket. All experiments were carried out with a constant axial shortening velocity of 1.0 μm/s (equivalent to a slip velocity of 1.15 μm/s along the fault surface) and with a constant confining pressure of 150 MPa at room temperature. In each experiment, after the shear stress reached a steady-state at an axial displacement of 0.7 to 1.1 mm, pore pressure changed abruptly. Initial values of P_p ranged from 50 to 100 MPa, and the magnitude of the step changes in P_p ranged from 7.8 to 71.0 MPa. These pressure measurements were accurate to ±0.06 MPa, and the step changes in P_p were accomplished in <0.3 s.

The friction coefficient (μ) is defined as:

$$\tau = \mu\sigma_e = \mu\left(\sigma_n - \alpha P_p\right) \tag{1}$$

where τ is the shear stress, σ_e the effective normal stress, σ_n the normal stress, α a constant, and P_p the pore pressure. The term α can be approximated by unity (Dieterich and Kilgore, 1994; Paterson and Wong, 2005), because it is related to the boundary porosity (i.e., the ratio between the true contact area and the apparent area on the slip surface in the friction behaviors). In our experiments, μ was calculated as follows:

$$\mu = \frac{\tau}{\sigma_e} = \frac{\sigma_{dif}\sin\theta\cos\theta}{\sigma_{dif}\sin^2\theta + P_c - \alpha P_p} \tag{2}$$

where σ_{dif} is the differential stress and θ is the angle of the oblique fault surfaces of the specimens (i.e., 30°). The mechanical data of the experiments were corrected to account for the strength of the jackets during deformation, and for the elastic shortening/extension along the axis caused by the stiffness of the apparatus (196 kN/mm).

3. Experimental results

Fig. 2 shows (a) pore pressure (P_p), and (b) shear stress (τ) and effective normal stress (σ_e), plotted as functions of slip displacement for a single series of experiment GR611, under wet conditions. The shear stress changed significantly and attained a new steady-state condition following the injection or ejection of the pore fluid. This mechanical response corresponds to the change in effective normal stress (Fig. 2). At high P_p (low σ_e), an unstable drop in shear stress (Hong and Marone, 2005) was occasionally observed before the next steady-state condition was attained (e.g. the steps at slip displacements of 1.8 and 4.3 mm in Fig. 2; see also Table 1, which summarizes the results of all experiments). These unstable stress drops occurred when σ_e was less than ca. 20 MPa. The steady-state shear strength of the antigorite serpentinite under wet conditions showed an almost linear dependence on the effective normal stress, and the friction coefficient was estimated as $\mu = 0.51 \pm 0.01$ from this slope

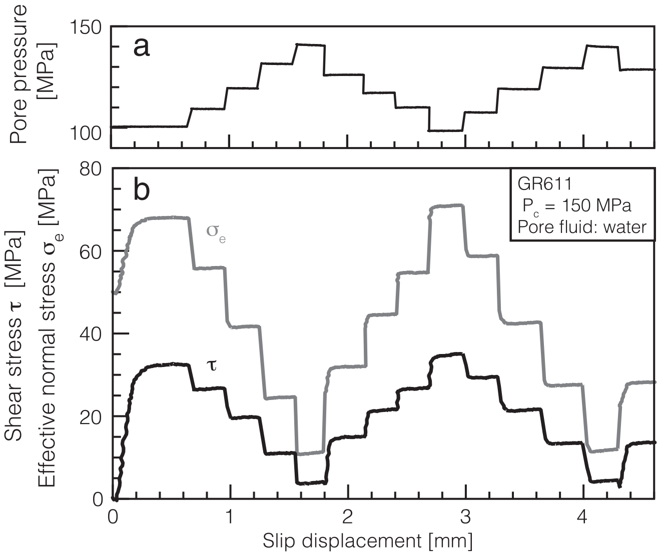

Fig. 2. Response of (a) imposed pore pressure history, and (b) shear stress and effective normal stress to changing slip displacement during a wet experiment (GR611). The confining pressure and slip velocity remained constant at 150 MPa and 1.15 μm/s, respectively. Pore pressure changed instantaneously and shear stress showed a rapid response to the change in pore pressure (effective normal stress). Shear stress, effective normal stress, and the friction coefficient history are shown in Table 1.